Observation of multi-scale turbulence and non-local transport in LHD plasmasa)

T. Tokuzawa, S. Inagaki, K. Ida, K. Itoh, T. Ido, A. Shimizu, H. Takahashi, S. Kitajima, N. Tamura, M. Yoshinuma, H. Tsuchiya, I. Yamada, K. Tanaka, T. Akiyama, Y. Nagayama, K. Kawahata, K. Y. Watanabe, H. Yamada, and LHD Experiment Group

Citation: Physics of Plasmas (1994-present) **21**, 055904 (2014); doi: 10.1063/1.4876619
View online: http://dx.doi.org/10.1063/1.4876619
View Table of Contents: http://scitation.aip.org/content/aip/journal/pop/21/5?ver=pdfcov
Published by the AIP Publishing

Observation of multi-scale turbulence and non-local transport in LHD plasmas[a)]

T. Tokuzawa,[1,2,b),c)] S. Inagaki,[2,3] K. Ida,[1,3] K. Itoh,[1,3] T. Ido,[1] A. Shimizu,[1] H. Takahashi,[1] S. Kitajima,[4] N. Tamura,[1] M. Yoshinuma,[1] H. Tsuchiya,[1] I. Yamada,[1] K. Tanaka,[1] T. Akiyama,[1] Y. Nagayama,[1] K. Kawahata,[1] K. Y. Watanabe,[1] H. Yamada,[1] and LHD Experiment Group[1]

[1]*National Institute for Fusion Science, Toki 509-5292, Japan*
[2]*Research Institute for Applied Mechanics, Kyushu University, Kasuga, Fukuoka 816-8580, Japan*
[3]*Itoh Research Center for Plasma Turbulence, Kyushu University, Kasuga, Fukuoka 816-8580, Japan*
[4]*Tohoku University, Aobayama 6-6-01-2, Sendai 980-8579, Japan*

(Received 29 December 2013; accepted 21 April 2014; published online 14 May 2014)

We have studied two types of spatio-temporal turbulence dynamics in plasmas in the Large Helical Device, based on turbulence measurements with high spatial and temporal resolution. Applying conditional ensemble-averaging to a plasma with Edge-Localized Modes (ELMs), fast radial inward propagation of a micro-scale turbulence front is observed just after ELM event, and the propagation speed is evaluated as ~100 m/s. A self-organized radial electric field structure is observed in an electrode biasing experiment, and it is found to realize a multi-valued state. The curvature of the radial electric field is found to play an important role for turbulence reduction.
 [http://dx.doi.org/10.1063/1.4876619]

I. INTRODUCTION

A spatio-temporal turbulence dynamics is one of the hot topics in the magnetic confined fusion plasma researches. The recent progress on the study of the meso-scale structures (such as zonal flows,[1,2] Geodesic Acoustic Modes (GAMs),[3–5] and streamers[6–8]) gives us that they are nonlinearly generated by micro-scale turbulences. The magneto-hydrodynamics (MHD) modes are also found to interact with micro-scale turbulences.[9] These interactions play an important role for transport physics. For the clarification of the puzzles which micro-, meso-, and macro-scale turbulences are coexisted and influenced each other, the study of "global dynamics," in other words "multi-scale interaction," is important. In addition, the studies of relation between heat/particle/momentum flux and temperature/density/flow gradient are shown that the flux is not necessarily determined by the local plasma parameters.[10–17] In cold pulse propagation experiments, for example, the core plasma temperature shows the fast change after the edge cooling.[18–20] The change of temperature is much faster than the expected value from the diffusive process in a thermal transport. It is considered that some linkages between edge and core. This phenomenon is called as non-local transport and the mechanism is still under discussion. One of the candidates is that the coupling with micro-scale turbulence and meso- or macro-scale turbulence forces the influence to the plasma parameters at separated radii. In this sense, one of the important experimental observations is the long range correlation fluctuation in the Large Helical Device (LHD).[21,22] In this observation, the low frequency electron temperature fluctuation is found to have a long radial correlation length. A nonlinear coupling with micro-scale turbulence and macro-scale low frequency fluctuation is clearly identified. This kind of linkage is used for the study of several interesting physical phenomena which include not only non-local phenomena but also widely seen common dynamic phenomena (such as collapse, transition, and transport). From this point of view, we try to apply the analysis of global dynamic of turbulence.

For this spatio-temporal dynamics study, the global observation of turbulence is necessary. Recently, multi channel Doppler back scattering (DBS) system has been installed in LHD.[23] DBS diagnostics has a potential to measure the radial electric field E_r and the density fluctuation intensity, simultaneously.[24,25] A multi-channel system can measure the profile of the interest parameters with high temporal resolution.[26] Currently, LHD DBS multi-channel system utilizes seven channels in Ka-band and the measured range of wave number is around 2–6 cm^{-1}. The ordinary or extra-ordinary polarization wave is selectable for matching the LHD experiment condition such as the magnetic field strength and the electron density.

The organization of this paper is as follows. In Sec. II, the observation of micro-scale turbulence propagation at the Edge-Localized Mode (ELM) events is described. In general, ELM event is a sort of the collapse phenomena and MHD bursts occur in the macro-scale.[27] The radial inward propagation of turbulence lump is observed at the same time. In Sec. III, micro- and meso-scale interaction in an electrode biasing experiment is explained. This experiment is a sort of transition phenomena. The concentration and reduction of turbulence related with E_r curvature are observed. In addition, the observation of a solitary localized E_r structure is obtained in the view of large scale. Summary is given in the final section.

[a)]Paper KI3 1, Bull. Am. Phys. Soc. **58**, 185 (2013); Invited paper (KI3.00001) of 55th Annual Meeting of the APS Division of Plasma Physics, Denver, Colorado, November 2013.
[b)]Invited speaker.
[c)]Electronic mail: tokuzawa@nifs.ac.jp

II. MICRO-SCALE TURBULENCE PROPAGATION

Radial propagation of micro-scale turbulence has been observed in plasmas with ELM events. ELM events have been sometimes observed in H-mode[28] plasma experiments in LHD.[29] The experiments are carried out in the magnetic configuration, where the magnetic axis position in the vacuum field is $R_{ax} = 3.9$ m, on-axis magnetic field strength is $B_t = 0.8$ T. Typical time evolutions of plasma parameters are shown in Fig. 1. In this discharge, the plasma is heated by neutral beam injectors (NBI), in which total power is around 10 MW. H_α signal[30] is a good indicator to notify onset of the ELM event and the ELM frequency is found to be around 70 Hz. These ELM events are considered as a sort of resistive interchange mode from the former study.[29] It makes the loss of about 10% of stored energy in this analyzing data set. When the ELM events occur, the line integrated electron density, which is measured by the 13-channel FIR interferometer system[31] drops just inside the last closed flux surface (LCFS) and increases outside. Figure 2 shows the radial profiles of electron density and temperature, which are measured by the Thomson scattering system.[32] Here, two time slices, which are before and after onset of ELM events, are shown. The measured timings, shown as a vertical line in Fig. 1, are corresponded with the probing laser injection timing. It is clearly observed that there is the pivot point and it locates around at LCFS. Now, the question is that the density at well

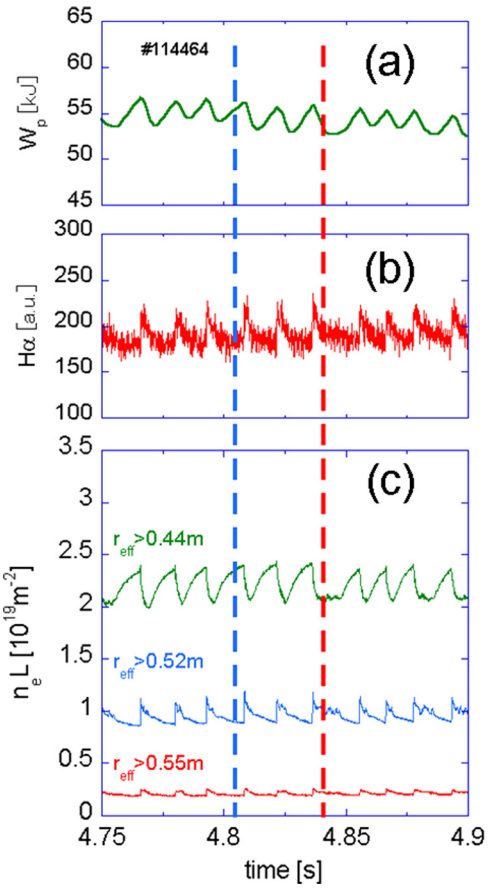

FIG. 1. Typical time evolutions of (a) stored energy, (b) Hα, and (c) line integrated density at ELM events. Here, the vertical dashed lines show the observation timing of Thomson scattering system.

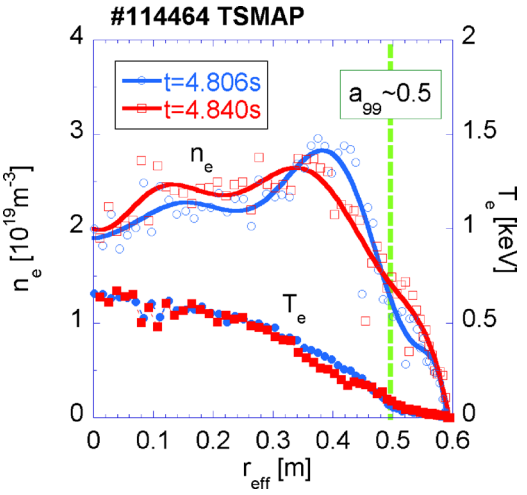

FIG. 2. Radial profiles of electron density and temperature measured by Thomson scattering system before (blue circle) and after ELM event (red rectangular). The effective LCFS is also shown vertical green line ($r_{eff} = a_{99}$, where 99% of the kinetic energy is confined).

inside of LCFS (about 10 cm) looks like also dropping, simultaneously. The propagation time scale is faster than the diffusive transit time scale. Some other physics probably play a role of this abrupt loss mechanism. We try to investigate the turbulence effect and pay attention to the happening of the turbulence near the pivot point.

ELM events are self-organized plasma phenomena and we utilize the statistical study by the conditional averaging technique. H_α signal is used as the indicator of ELM events and the onset of ELM events is expressed as $t =$ zero as shown in Fig. 3(a). Here, 146 events are used for this analysis. The magnetic fluctuation is observed by Mirnov coils[33] as shown in Fig. 3(b). It shows that the MHD event occurs during very short time (less than 0.5 ms) and it might be a trigger of the turbulence burst. The high frequency density fluctuation amplitude, which has over 100 kHz frequency components, is evaluated by applying a short-time fast

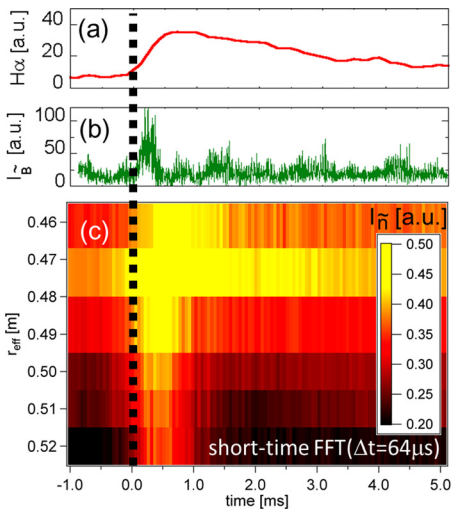

FIG. 3. Time evolutions of the ensemble averaged (a) Hα signal and (b) magnetic fluctuation intensity. (c) Contour map of the change of the high frequency density fluctuation component versus effective radius and time. Each time window is 64μs and ensemble-averaging number is 146.

Fourier transform (FFT) to each DBS signal. Contour map of the temporal change of turbulence amplitude versus effective radius is shown in Fig. 3(c). Here, each time window is 64 μs and 146 events are ensemble-averaged. Just after the ELM onset, rapid increase of turbulence amplitude at 2 cm inside the pivot point is observed. Then, the turbulence front looks like propagate inward direction with a fast time scale.

Before the detailed description of the phenomena, we discuss about the ambiguity. In order to establish the unambiguous observation of the temporal turbulence amplitude changes, the statistical convergence analysis is performed with respect to peaks observed in the time evolution of the fluctuation amplitude. Figure 4 shows the amplitude of the changes as a function of the number of ensemble N (i.e., the number of observed ELM events). The variations are defined as the difference between the mean values during -0.5 to -0.1 ms and $+0.1$ to $+1.0$ ms, respectively. In the limit of $N \rightarrow \infty$, the variations converge to the finite values. Thus, the temporal change in fluctuation amplitude discussed here is not a random variation but the unambiguous dynamical change at the onset of ELM event. One can conclude that the averaging by use of 146 observations provides a significant data set for the analysis.

The propagation of a micro-scale turbulence front in space is clearly illustrated as follows. The envelope of high frequency component of each DBS signal is able to use as the indicator, since it has the information of temporal behavior of turbulence intensity. Figure 5 shows the time evolution of the distinct turbulence intensity at each radial position. Here, upper two time traces show the behavior at inside the pivot point and the others are outside. The front of turbulence burst is travelling from the pivot point radially by a distance several times of ion sound radius ($\rho_s \sim 3$ mm), propagating inward at a speed of $\sim$100 m/s. This fast turbulence propagation may cause a drop in density as far as 10 cm inside of the LCFS. In future for this phenomenon study, a gradient propagation time scale will be compared with a turbulence propagation speed. We here comment about the change of bulk component. The "mean" density, that is a bulk component, is also changed at ELM event but its response time is slightly slow (>1 ms) and it does not affect the conclusion of this analysis.

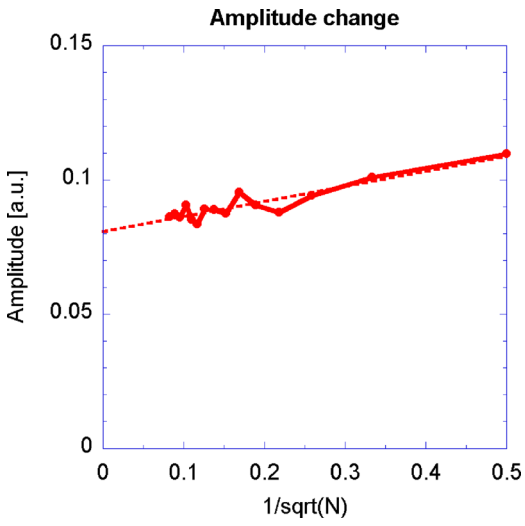

FIG. 4. Convergence analysis of the amplitude of the changes observed at $r_{\mathrm{eff}} \sim 0.48$ [m].

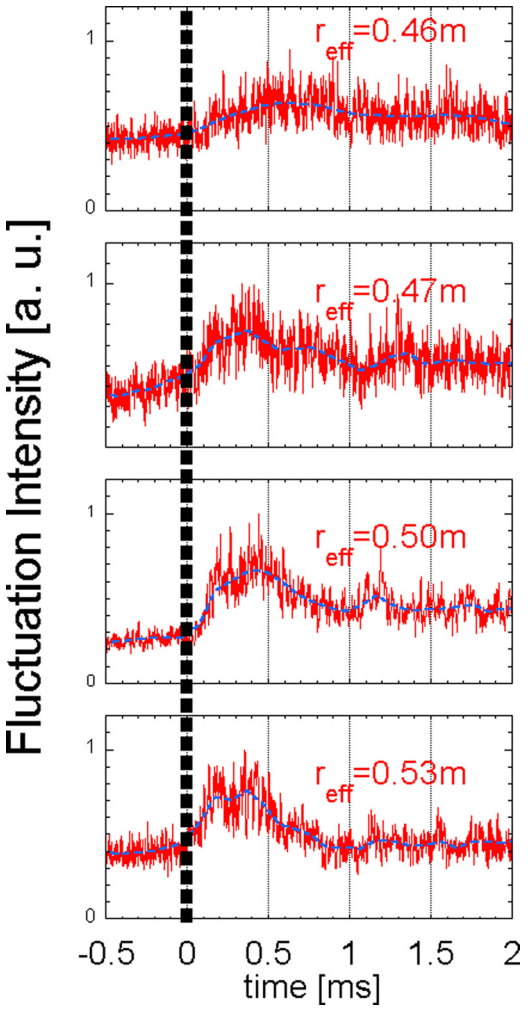

FIG. 5. Temporal behaviors of density fluctuation intensity through the high pass filter over 100 kHz.

III. MESO- AND MICRO-SCALE INTERACTION

We investigate the interaction between radial electric field E_r and density fluctuation in transient plasma experiments. Some former fusion plasma experiments show that the transport barrier phenomena such as L-H transition are strongly related with the local electric field but the barrier location does not completely match with the E_r maximum location nor the maximum E_r shear location.[33,34] It is still under a question but the turbulence might play a role. Theoretical prediction of the turbulence intensity is expressed by $\frac{\partial I}{\partial t} = \gamma I - \omega_2 I^2 - \alpha(-E_r E''_r)I$.[35,36] Here, I is the turbulence intensity, γ is the growth rate, ω_2 is the non-linear damping rate, $\alpha(-E_r E''_r)$is the flow intensity component, and E_r'' is the curvature of E_r. According to this expectation, simultaneous observation of both Er and turbulence will give us new information.

The experiment is carried out in the electrode biasing experiment in LHD.[37] Main issue of this electrode biasing experiment itself is the control of the $\boldsymbol{J} \times \boldsymbol{B}$ driving force for

a poloidal plasma rotation externally. Here, $\boldsymbol{J}$ and $\boldsymbol{B}$ are a biasing electrode current and a magnetic field. It is suitable experiment for the study of bifurcation phenomena of transition. In this experiment, the center of the electrode is inserted to $r_{\rm eff}/a_{99} \sim 0.8$. The electrode is connected to the vacuum vessel through the dc power supply and now positively biased against the vacuum vessel.

The target plasma is produced by ECH with 0.8 MW in the magnetic configurations where the magnetic axis position in the vacuum field is $R_{\rm ax} = 3.75$ m, and the magnetic field strength is $B_{\rm t} = 1.375$ T. The multi-channel DBS is used for measuring the profile of edge poloidal flow velocity V_θ (and $E_{\rm r}$) and fluctuation amplitude. Figures 6(b) and 6(c) show the time evolutions of the electrode current ($I_{\rm E}$) and the electrode applied voltage ($V_{\rm E}$), respectively. The electrode current gradually increases according to the increase of bias voltage. The current suddenly drops down at around $t = 4.22$ s and rises up at $t = 4.46$ s. It is considerable that the negative resistance phenomenon is appeared and the forward and the reverse transition are occurred. During this phenomenon, the radial profiles of V_θ are measured around the electrode by DBS as shown in Fig. 6(a). At first, the poloidal velocity starts to increase near the electrode ($r_{\rm eff} \sim 0.48$). Just after the forward transition, the strong flow region moves to outward. Then, it comes back near the electrode just before the back transition. The observed poloidal velocity is expressed by the sum of the $\boldsymbol{E} \times \boldsymbol{B}$ velocity and the phase velocity of turbulence, that is $V_\theta = V_{\boldsymbol{E}\times\boldsymbol{B}} + V_{\rm phase}$. Now, we estimate the value of $E_{\rm r}$ from the observed poloidal velocity.

Temporal behavior of the estimated $E_{\rm r}$ profile is almost similar with the poloidal velocity. During the transition and ramp-up phase of bias voltage ($t = 4.28$–4.38 s), the $E_{\rm r}$ structures are changing as shown in Fig. 7. At first, a solitary peaked structure is observed and then the peak position moves outward as a time. In addition, a double peak structure appears

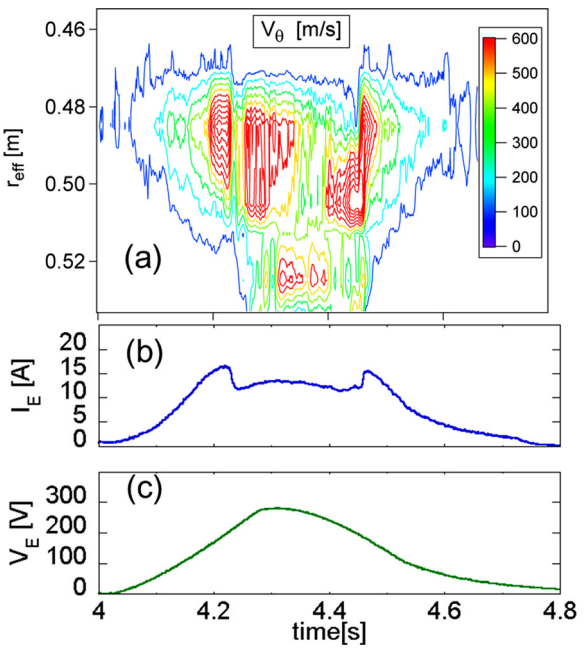

FIG. 6. (a) Contour map of poloidal velocity versus effective radius and time. Time evolutions of (b) electrode current and (c) applied bias voltage.

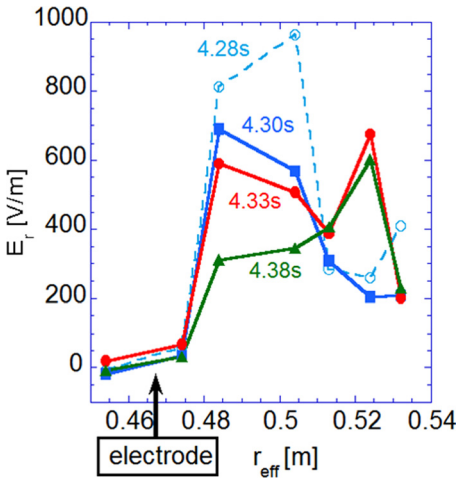

FIG. 7. Radial profile of the estimated radial electric field.

in transiently. Such kind of multi-peak $E_{\rm r}$ structures were predicted in the theory,[38] which describes about $E_{\rm r}$ bifurcation on the electrode biasing effect. The solitary structure with multiple peaks has been derived. The model, however, is calculated for limiter configuration tokamak plasmas. Future study is expected for applying our current LHD configuration that has a natural divertor with no-limiter and a complicated three-dimensional configuration. Therefore, it is newly found that a self-organized $E_{\rm r}$ is producing and multi-valued state of $E_{\rm r}$ is realizing in LHD plasmas.

Theoretical prediction[35,36] says the meso-scale mean flow $\alpha(-E_r E''_r)$ affect the turbulence and now we compare the profiles of the turbulence with the $E_{\rm r}$ related value. The turbulence intensity is evaluated by the summation of high frequency (>100 kHz) components in DBS scattering signal

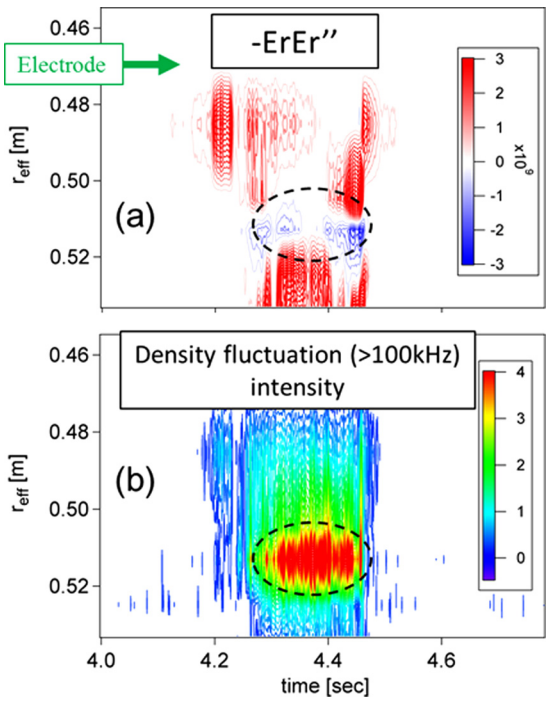

FIG. 8. Contour map of (a) the estimated value of $-E_r E''_r$ and (b) the intensity of high frequency fluctuation component.

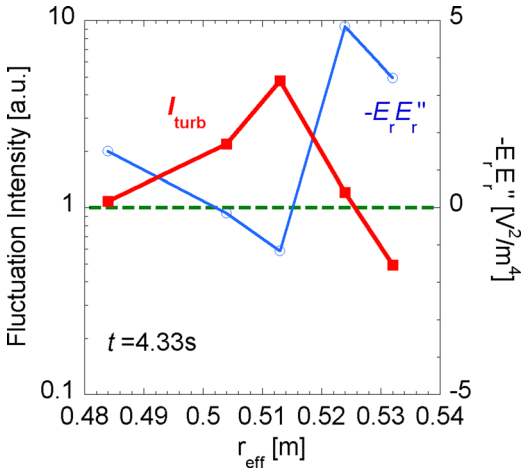

FIG. 9. Radial profiles of the turbulence intensity (red rectangular) and the estimated value of $-E_r E_r''$ (blue circle) at $t = 4.33$ s.

amplitude. The calculated spatio-temporal behavior of turbulence intensity is shown by the contour map in Fig. 8(b). Turbulence intensity seems to be localized in around $r_{\rm eff} = 0.51$ during the transition period. Figure 8(a) shows the calculated value of $-E_r\, E_r''$. Here, the color of red means positive value and the blue color means the negative. Intensity of turbulence looks like strong in the negative region of $-E_r\, E_r''$ in space and time. At the time slice of $t = 4.33$ s, the radial profiles of both turbulence intensity and $-E_r\, E_r''$ are shown in Fig. 9. Concentration of turbulence intensity is correlated with negative region of $-E_r\, E_r''$. This result is not conflict with the theoretical hypothesis which says "turbulence reduction/concentration is trapping a through or summit according to the sign of E_r". Therefore, it is found that the meso-scale parameters of E_r and also E_r'' are important for reduction of micro-scale turbulence.

IV. SUMMARY

Recent experimental observations of multi-scale turbulence by the microwave diagnostics of multi-channel DBS with high spatial and temporal resolution have been analyzed in LHD. In the ELM event plasma experiments, the fast radial inward propagation of a micro-scale turbulence front is observed. The propagation speed is estimated around 100 m/s. This front dynamics of turbulence propagation may cause a drop in density deep inside of the LCFS. The statistical convergence is checked for applying of the conditional ensemble-averaging technique and the use of 146 observations is found to be a significant data set. In the electrode biasing experiment, the radial profile of poloidal flow velocity is obtained around the inserting electrode and a self-organized E_r (multi-valued state of E_r) is observed. Simultaneous multi point measurements of E_r and turbulence intensity lead that the curvature of E_r (that is E_r'') might play an important role for turbulence reduction.

ACKNOWLEDGMENTS

The authors thank Professor S.-I. Itoh and Professor N. Kasuya for useful discussion. This work was partly supported by KAKENHI (Nos. 21224014, 22360394, 23244113, 23360414, and 25289342) and by the collaboration programs of NIFS (NIFS10KOAP023, NIFS13KOCT001) and of the RIAM of Kyushu University and Asada Science foundation. Also, this work was supported by Japan/U.S. Cooperation in Fusion Research and Development.

[1]A. Fujisawa, Nucl. Fusion **49**, 013001 (2009).
[2]P. H. Diamond, S.-I. Itoh, K. Itoh, and T. S. Hahm, Plasma Phys. Controlled Fusion **47**, R35 (2005).
[3]A. Fujisawa, K. Itoh, H. Iguchi, K. Matsuoka, S. Okamura, A. Shimizu, T. Minami, Y. Yoshimura, K. Nagaoka, C. Takahashi, M. Kojima, H. Nakano, S. Ohsima, S. Nishimura, M. Isobe, C. Suzuki, T. Akiyama, K. Ida, K. Toi, S.-I. Itoh, and P. H. Diamond, Phys. Rev. Lett. **93**, 165002 (2004).
[4]Y. Nagashima, K. Itoh, S.-I. Itoh, A. Fujisawa, M. Yagi, K. Hoshino, K. Shinohara, A. Ejiri, Y. Takase, T. Ido, K. Uehara, Y. Miura, and JFT-2M Group, Plasma Phys. Controlled Fusion **49**, 1611 (2007).
[5]K. Hallatschek and D. Biskamp, Phys. Rev. Lett. **86**, 1223 (2001).
[6]T. Yamada, S.-I. Itoh, T. Maruta, N. Kasuya, Y. Nagashima, S. Shinohara, K. Terasaka, M. Yagi, S. Inagaki, Y. Kawai, A. Fujisawa, and K. Itoh, Nature Phys. **4**, 721 (2008).
[7]J. F. Drake, A. Zeiler, and D. Biskamp, Phys. Rev. Lett. **75**, 4222 (1995).
[8]S. Champeaux and P. Diamond, Phys. Lett. A **288**, 214 (2001).
[9]W. X. Ding, D. L. Brower, D. Craig, B. H. Deng, S. C. Prager, J. S. Sarff, and V. Svidzinski, Phys. Rev. Lett. **99**, 055004 (2007).
[10]L. Laurent, Plasma Phys. Controlled Fusion **28**, 85 (1986).
[11]E. D. Fredrickson, K. McGuire, A. Cavallo, R. Budny, A. Janos, D. Monticello, Y. Nagayama, W. Park, G. Taylor, and M. C. Zarnstorff, Phys. Rev. Lett. **65**, 2869 (1990).
[12]J. G. Cordey, D. G. Muir, S. V. Neudatchin, V. V. Parail, S. Ali-Arshad, D. V. Bartlett, D. J. Campbell, A. E. Costley, A. L. Colton, A. W. Edwards, L. Porte, A. C. C. Sips, E. M. Springmann, P. M. Stubberfield, G. Vayakis, M. G. von Hellermann, A. Taroni, and K. Thomsen, Plasma Phys. Controlled Fusion **36**, A267 (1994).
[13]U. Stroth, L. Giannone, H. J. Hartfuss, ECH Group, and W7-AS Team, Plasma Phys. Controlled Fusion **38**, 611 (1996).
[14]S. Inagaki, N. Tamura, K. Ida, K. Tanaka, Y. Nagayama, K. Kawahata, S. Sudo, K. Itoh, S.-I. Itoh, A. Komori, and LHD Experimental Group, Plasma Phys. Controlled Fusion **52**, 075002 (2010).
[15]S. Inagaki, T. Tokuzawa, N. Tamura, S.-I. Itoh, T. Kobayashi, K. Ida, T. Shimozuma, S. Kubo, K. Tanaka, T. Ido, A. Shimizu, H. Tsuchiya, N. Kasuya, Y. Nagayama, K. Kawahata, S. Sudo, H. Yamada, A. Fujisawa, K. Itoh, and LHD Experiment Group, Nucl. Fusion **53**, 113006 (2013).
[16]K. Ida, Y. Sakamoto, H. Takenaga, N. Oyama, K. Itoh, M. Yoshinuma, S. Inagaki, T. Kobuchi, A. Isayama, T. Suzuki, T. Fujita, G. Matsunaga, Y. Koide, M. Yoshida, S. Ide, Y. Kamada, and JT-60 Team, Phys. Rev. Lett. **101**, 055003 (2008).
[17]K. Ida, Z. Shi, H. Sun, S. Inagaki, K. Kamiya, J. Rice, N. Tamura, P. H. Diamond, T. Estrada, C. Hidalgo, X. L. Zou, G. Dif-Pradalier, T. S. Hahm, U. Stroth, A. Field, K. Itoh, X. Ding, J. Dong, S. I. Itoh, Y. Sakamoto, and S. Oldenburger, in Proceedings of the 24th International Conference on Fusion Energy, San Diego, 2012 [OV/3-4], see http://www-naweb.iaea.org/napc/physics/FEC/FEC2012/index.htm.
[18]M. W. Kissick, E. D. Fredrickson, J. D. Callen, C. E. Bush, Z. Chang, P. C. Efthimion, R. A. Hulse, D. K. Mansfield, H. K. Park, J. F. Schivell, S. D. Scott, E. J. Synakowski, G. Taylor, and M. C. Zarnstorff, Nucl. Fusion **34**, 349 (1994).
[19]K. W. Gentle, W. L. Rowan, R. V. Bravenec, G. Cima, T. P. Crowley, H. Gasquet, G. A. Hallock, J. Heard, A. Ouroua, P. E. Phillips, D. W. Ross, P. M. Schoch, and C. Watts, Phys. Rev. Lett. **74**, 3620 (1995).
[20]N. Tamura, S. Inagaki, K. Ida, T. Shimozuma, S. Kubo, T. Tokuzawa, K. Tanaka, S. V. Neudatchin, K. Itoh, D. Kalinina, S. Sudo, Y. Nagayama, K. Ohkubo, K. Kawahata, A. Komori, and LHD Experimental Group, Phys. Plasmas **12**, 110705 (2005).
[21]S. Inagaki, T. Tokuzawa, K. Itoh, K. Ida, S.-I. Itoh, N. Tamura, S. Sakakibara, N. Kasuya, A. Fujisawa, S. Kubo, T. Shimozuma, T. Ido, S. Nishimura, H. Arakawa, T. Kobayashi, K. Tanaka, Y. Nagayama, K. Kawahata, S. Sudo, H. Yamada, A. Komori, and LHD Experiment Group, Phys. Rev. Lett. **107**, 115001 (2011).

[22]K. Itoh, S.-I. Itoh, S. Inagaki, T. Kobayashi, A. Fujisawa, Y. Nagashima, S. Oldenbürger, K. Ida, T. Tokuzawa, Y. Nagayama, K. Kawahata, H. Yamada, and LHD Experiment Group, Plasma Phys. Controlled Fusion **54**, 095016 (2012).
[23]T. Tokuzawa, Plasma Fusion Res (submitted); paper presented at the 11th International Reflectometry Workshop (Palaiseau, France, 2013), see http://www.aug.ipp.mpg.de/IRW/.
[24]G. D. Conway, B. Scott, J. Schirmer, M. Reich, A. Kendl, and ASDEX Upgrade Team, Plasma Phys. Controlled Fusion **47**, 1165 (2005).
[25]T. Happel, E. Blanco, and T. Estrada, Rev. Sci. Instrum. **81**, 10D901 (2010).
[26]W. A. Peebles, T. L. Rhodes, J. C. Hillesheim, L. Zeng, and C. Wannberg, Rev. Sci. Instrum. **81**, 10D902 (2010).
[27]J. W. Connor, Plasma Phys. Controlled Fusion **40**, 531 (1998).
[28]F. Wagner, G. Becker, K. Behringer, D. Campbell, A. Eberhagen, W. Engelhardt, G. Fussmann, O. Gehre, J. Gernhardt, G. Gierke, G. Haas, M. Huang, F. Karger, M. Keilhacker, O. Klüber, M. Kornherr, K. Lackner, G. Lisitano, G. G. Lister, H. M. Mayer, D. Meisel, E. R. Müller, H. Murmann, H. Niedermeyer, W. Poschenrieder, H. Rapp, H. Röhr, F. Schneider, G. Siller, E. Speth, A. Stäbler, K. H. Steuer, G. Venus, O. Vollmer, and Z. Yü, Phys. Rev. Lett. **49**, 1408 (1982).
[29]K. Toi, F. Watanabe, S. Ohdachi, S. Morita, X. Gao, K. Narihara, S. Sakakibara, K. Tanaka, T. Tokuzawa, H. Urano, A. Weller, I. Yamada, L. Yan, and LHD Experiment Group, Fusion Sci. Technol. **58**, 61 (2010).
[30]M. Goto, S. Morita, H. Y. Zhou, C. F. Dong, and LHD Experiment Group, Fusion Sci. Technol. **58**, 394 (2010).
[31]T. Akiyama, K. Kawahata, K. Tanaka, T. Tokuzawa, Y. Ito, S. Okajima, K. Nakayama, C. A. Michael, L. N. Vyacheslavov, A. Sanin, S. Tsuji-Iio, and LHD Experiment Group, Fusion Sci. Technol. **58**, 352 (2010).
[32]I. Yamada, K. Narihara, H. Funaba, T. Minami, H. Hayashi, T. Kohmoto, and LHD Experiment Group, Fusion Sci. Technol. **58**, 345 (2010).
[33]S. Sakakibara, H. Yamada, and LHD Experiment Group, Fusion Sci. Technol. **58**, 471 (2010).
[34]R. A. Moyer, K. H. Burrell, T. N. Carlstrom, S. Coda, R. W. Conn, E. J. Doyle, P. Gohil, R. J. Groebner, J. Kim, R. Lehmer, W. A. Peebles, M. Porkolab, C. L. Rettig, T. L. Rhodes, R. P. Seraydarian, R. Stockdale, D. M. Thomas, G. R. Tynan, and J. G. Watkins, Phys. Plasmas **2**, 2397 (1995).
[35]K. Kamiya, Y. Sakamoto, G. Matsunaga, A. Kojima, H. Urano, N. Oyama, Y. Koide, Y. Kamada, K. Ida, T. Kurki-Suonio, and JT-60 Team, Nucl. Fusion **51**, 053009 (2011).
[36]K. Itoh, S.-I. Itoh, M. Yagi, and A. Fukuyama, J. Plasma Fus. Res. Ser. **8**, 119 (2009).
[37]S. Kitajima, H. Takahashi, K. Ishii, Y. Sato, M. Kanno, J. Tachibana, A. Okamoto, M. Sasao, S. Inagaki, M. Takayama, S. Masuzaki, M. Shoji, N. Ashikawa, M. Tokitani, M. Yokoyama, Y. Suzuki, S. Satake, T. Ido, A. Shimizu, C. Suzuki, Y. Nagayama, T. Tokuzawa, K. Nishimura, T. Morisaki, and LHD Experiment Group, Nucl. Fusion **53**, 073014 (2013).
[38]N. Kasuya, K. Itoh, and Y. Takase, Nucl. Fusion **43**, 244 (2003).